Pure Appl. Geophys. 173 (2016), 2671–2686

DOI 10.1007/s00024-016-1349-1

Pure and Applied Geophysics

Does Biot's theory have predictive power?

Igor A. Beresnev[1]

Abstract—Biot's theory of elastic waves in fluid-saturated porous solids has two free parameters: the tortuosity α, characterizing the dynamic coupling between the solid and the fluid, and the structural factor δ, representing the geometric properties of the porous space. The meaning and significance of these parameters have not been sufficiently understood. The tortuosity has the physical meaning of the normalized mean square of the velocity of the pore fluid relative to the solid wall; it has a low-frequency but no high-frequency limits. The analytical calculation of the tortuosity for Biot's slit-like pore provides its range of variability from approximately 1–100 in the frequency range of practical interest. The tortuosity has a significant effect on the properties of the Biot waves of the second kind in the high-frequency range. On the other hand, in realistically complex pore geometries, the values of the tortuosity are virtually unpredictable. This limits the usefulness of the Biot theory in predicting the wave propagation at high frequencies. At all frequencies, the effect of the structural factor is insignificant relative to the effect of the tortuosity. The conventional compressional wave (the wave of the first kind) is insensitive to both parameters at all frequencies. The frequencies of interest to seismic exploration are also free of the uncertainty imposed by the lack of constraints on the tortuosity as the only free parameter in Biot's theory.

Key words: Biot theory, Elastic waves, Porous media, Tortuosity.

1. Introduction

The classic theory of elastic-wave propagation in a fluid-saturated porous solid was established by Biot (1956a, b). The elastic constants of the theory are P, Q, R, and μ_{fr}, where μ_{fr} is the shear modulus of the dry porous frame, and P, Q, and R are fully determined through the bulk moduli of the pure solid K_0 and the pure fluid K_f, the bulk modulus of the dry frame K_{fr}, and the porosity φ (e.g., Mavko et al. 2009, p. 266). In writing the expression for the kinetic energy per unit volume of the aggregate, Biot also had to postulate three additional "induced-mass" coefficients ρ_{11}, ρ_{12}, ρ_{22} arising from the dynamic coupling between the solid and the fluid (Biot 1956a, Eq. 3.2). However, Biot offered no clear recipe for finding these coefficients. It is also worth noting that Biot's induced-mass coefficients are not the same as the components of the induced-mass tensor introduced in fluid mechanics to describe the flow past solid bodies. The expression for the kinetic energy defining Biot's ρ_{11}, ρ_{12}, ρ_{22} involves the velocity components of both the fluid and the solid, whereas the kinetic energy used to define the induced-mass tensor is expressed through the velocities of the moving body only (cf. Biot 1956a, Eq. 3.2 and Landau and Lifshitz 1959, Eq. 11.4).

Expressions for determining ρ_{11}, ρ_{12}, and ρ_{22} through a single parameter α called "tortuosity" appeared in later literature,

$$\begin{aligned} \rho_{11} &= (1-\varphi)\rho_s - (1-\alpha)\rho_f, \\ \rho_{22} &= \alpha\varphi\rho_f, \\ \rho_{12} &= (1-\alpha)\varphi\rho_f, \end{aligned} \tag{1}$$

where ρ_s and ρ_f are the densities of the pure solid and pure fluid (e.g., Mavko et al. 2009, pp. 266–267, presented without derivation). Molotkov (2002) provided the derivation of this result based on the original definitions by Biot.

In extending the theory to the high-frequency range, Biot introduced the complex function $F(\kappa)$ describing the deviation of the friction force, exerted by the fluid on the pore wall, from its value in Poiseuillean flow, where κ is a non-dimensional frequency parameter (Biot 1956b, Eqs. 4.2, 4.3). The functional form of $F(\kappa)$ had to be postulated as

$$F(\kappa) = F\left[\delta(f/f_c)^{1/2}\right], \tag{2}$$

[1] Department of Geological and Atmospheric Sciences, Iowa State University, 253 Science I, 2237 Osborn Drive, Ames, IA 50011-3212, USA. E-mail: beresnev@iastate.edu

where f is the wave frequency, f_c is a characteristic frequency, and δ is an undetermined geometric parameter called the "structural factor" (Biot 1956b, Eq. 4.30). The two coefficients, the tortuosity α and the structural factor δ, became the free parameters of the Biot theory.

The nature of the coefficients α and δ and even the range of their possible values have not been well understood. It is the purpose of this paper to explore the effect of the tortuosity and the structural factor on the properties of the elastic waves in a fluid-saturated porous solid, the meaning of these coefficients, their measurability, and the limits of the Biot theory in predicting the properties of the propagating waves given the uncertainty in constraining the free parameters.

2. The velocity-dispersion equation

To analyze the dependence of the elastic-wave velocity on the tortuosity and the structural factor, we need to obtain the roots of the full velocity-dispersion equation in explicit form. For the compressional waves, which will be the focus of this study, the full dispersion relation valid at all frequencies is Eq. (6.3) of Biot (1956b). [The equation in the original contains a typo: the term $(\gamma_{11}\gamma_{22}-\gamma_{12})^2$ should read $(\gamma_{11}\gamma_{22}-\gamma_{12}^2)$]. Re-written through the elastic constants P, Q, R and the mass coefficients ρ_{11}, ρ_{12}, ρ_{22}, also using the definition of the characteristic frequency f_c (Biot 1956b, Eq. 4.8), the dispersion relation for the compressional waves becomes

$$\frac{PR-Q^2}{\rho^2}\frac{1}{V^4} - \left[\frac{R\rho_{11}+P\rho_{22}-2Q\rho_{12}}{\rho^2} - \frac{i\varphi\rho_f}{\rho}\frac{f_c}{f}F(\kappa)V_c^2\right]\frac{1}{V^2} + \left[\frac{\rho_{11}\rho_{22}-\rho_{12}^2}{\rho^2} - \frac{i\varphi\rho_f}{\rho}\frac{f_c}{f}F(\kappa)\right] = 0, \quad (3)$$

where $V=\omega/l$ is the complex velocity and l is the complex wavenumber, $\rho=\varphi\rho_f+(1-\varphi)\rho_s$ is the aggregate's density, $V_c^2=H/\rho$ is the reference velocity, and $H\equiv P+R+2Q$. Equation (3) is solved for $1/V^2$:

$$\frac{1}{V^2}=\frac{R\rho_{11}+P\rho_{22}-2Q\rho_{12}-i\varphi\rho_f H\frac{f_c}{f}F \pm \sqrt{\left(R\rho_{11}+P\rho_{22}-2Q\rho_{12}-i\varphi\rho_f H\frac{f_c}{f}F\right)^2-4(PR-Q^2)(\rho_{11}\rho_{22}-\rho_{12}^2-i\varphi\rho_f\rho\frac{f_c}{f}F)}}{2(PR-Q^2)}, \quad (4)$$

where the "plus" sign at the root is for the Biot "slow" wave (the wave of the second kind) and the "minus" is for the conventional "fast" wave (the wave of the first kind).

To make the expression for the velocity explicit and suitable for calculations, one needs to extract the square root in (4). The root can be represented as $\sqrt{a_1+ib_1}$, where

$$a_1 \equiv \left(R\rho_{11}+P\rho_{22}-2Q\rho_{12}+\varphi\rho_f H\frac{f_c}{f}F_i\right)^2 - 4\left(PR-Q^2\right)\left(\rho_{11}\rho_{22}-\rho_{12}^2+\varphi\rho_f\rho\frac{f_c}{f}F_i\right) - (\varphi\rho_f H\frac{f_c}{f}F_r)^2, \quad (5)$$

$$b_1 \equiv 2\varphi\rho_f\frac{f_c}{f}F_r\left[2(PR-Q^2)\rho - H\left(R\rho_{11}+P\rho_{22}-2Q\rho_{12}+\varphi\rho_f H\frac{f_c}{f}F_i\right)\right],$$

and F_r and F_i are the real and imaginary parts of the function $F(\kappa)$. The root is then explicitly written as (Abramowitz and Stegun 1964, Eq. 3.7.27)

$$(a_1+ib_1)^{1/2}=\pm\left[\left(\frac{r_1+a_1}{2}\right)^{1/2}+i(\mathrm{sign}b_1)\left(\frac{r_1-a_1}{2}\right)^{1/2}\right], \quad (6)$$

where r_1 is the modulus

$$r_1=(a_1^2+b_1^2)^{1/2}. \quad (7)$$

This replaces Eq. (4) with

$$\frac{1}{V^2}=\frac{R\rho_{11}+P\rho_{22}-2Q\rho_{12}-i\varphi\rho_f H\frac{f_c}{f}F\pm\frac{1}{\sqrt{2}}\left[(r_1+a_1)^{1/2}+i(\mathrm{sign}b_1)(r_1-a_1)^{1/2}\right]}{2(PR-Q^2)},$$

which, again, can be represented as $\frac{1}{V^2}=a_2+ib_2$, where

$$a_2\equiv\frac{R\rho_{11}+P\rho_{22}-2Q\rho_{12}+\varphi\rho_f H\frac{f_c}{f}F_i\pm\left(\frac{r_1+a_1}{2}\right)^{1/2}}{2(PR-Q^2)}, \tag{8}$$

$$b_2\equiv\frac{-\varphi\rho_f H\frac{f_c}{f}F_r\pm(\mathrm{sign}b_1)\left(\frac{r_1-a_1}{2}\right)^{1/2}}{2(PR-Q^2)}.$$

Extracting the square root one more time leads to the final expression for the complex velocity

$$\frac{1}{V}=\pm\left[\left(\frac{r_2+a_2}{2}\right)^{1/2}+i(\mathrm{sign}b_2)\left(\frac{r_2-a_2}{2}\right)^{1/2}\right] \tag{9}$$

where r_2 is the modulus

$$r_2=(a_2^2+b_2^2)^{1/2}. \tag{10}$$

The positive sign in (9) should be selected.

$$V^2=\frac{2(PR-Q^2)}{R\rho_{11}+P\rho_{22}-2Q\rho_{12}-i\varphi\rho_f H\frac{f_c}{f}F\pm\sqrt{\left(R\rho_{11}+P\rho_{22}-2Q\rho_{12}-i\varphi\rho_f H\frac{f_c}{f}F\right)^2-4(PR-Q^2)\left(\rho_{11}\rho_{22}-\rho_{12}^2-i\varphi\rho_f\rho\frac{f_c}{f}F\right)}},$$

Equation (9), combined with (1), (2), (5), (7), (8), and (10), can be used to calculate the complex velocity (or the complex wavenumber $l=\omega/V$) for the propagating compressional waves. The "plus" sign in (8) should be selected for the slow wave and "minus" for the fast wave.

The phase velocities are calculated as

$$c=\frac{\omega}{l_r}=\frac{1}{\mathrm{Re}\left(\frac{1}{V}\right)}=\left(\frac{2}{r_2+a_2}\right)^{1/2}, \tag{11}$$

where $l_r=\mathrm{Re}(l)$, with the same sign selection in (8) to pick the slow or the fast wave.

There is a practical difficulty in using Eq. (11) in the calculation of the fast-wave phase velocity. At relatively high values of porosity (greater than approximately 0.85), certain combinations of input parameters cause r_2 to become very close to the negative a_2, leading to a loss of precision and the numerical "underflow" (an artificial division by zero). Computations become unstable. This situation does not occur for the slow wave. The difficulty can be avoided if, for the fast-wave calculation, the original Eq. (4) is inverted, leading to

and then the numerator and denominator on the right-hand side are multiplied by

$$R\rho_{11}+P\rho_{22}-2Q\rho_{12}-i\varphi\rho_f H\frac{f_c}{f}F\mp\sqrt{\left(R\rho_{11}+P\rho_{22}-2Q\rho_{12}-i\varphi\rho_f H\frac{f_c}{f}F\right)^2-4(PR-Q^2)\left(\rho_{11}\rho_{22}-\rho_{12}^2-i\varphi\rho_f\rho\frac{f_c}{f}F\right)}.$$

This results in an alternative equation for the complex velocity,

$$V^2 = \frac{R\rho_{11} + P\rho_{22} - 2Q\rho_{12} - i\varphi\rho_f H\frac{f_c}{f}F \pm \sqrt{\left(R\rho_{11} + P\rho_{22} - 2Q\rho_{12} - i\varphi\rho_f H\frac{f_c}{f}F\right)^2 - 4(PR - Q^2)\left(\rho_{11}\rho_{22} - \rho_{12}^2 - i\varphi\rho_f\rho\frac{f_c}{f}F\right)}}{2\left(\rho_{11}\rho_{22} - \rho_{12}^2 - i\varphi\rho_f\rho\frac{f_c}{f}F\right)}, \tag{12}$$

where now the "minus" sign in the numerator stands for the slow wave and "plus" for the fast one.

The square root in Eq. (12) is the same as that in Eq. (4), and so expression (6) for it still holds, with the coefficients a_1, b_1, and r_1 still defined by (5) and (7). Using (6) to replace the root in (12) as before transforms Eq. (12) to $V^2 = a_2^* + ib_2^*$, with the new coefficients

$$a_2^* \equiv \frac{\left[R\rho_{11} + P\rho_{22} - 2Q\rho_{12} + \varphi\rho_f H\frac{f_c}{f}F_i \pm \left(\frac{r_1+a_1}{2}\right)^{1/2}\right]\left(\rho_{11}\rho_{22} - \rho_{12}^2 + \varphi\rho_f\rho\frac{f_c}{f}F_i\right) - \varphi\rho_f\rho\frac{f_c}{f}F_r\left[\pm(\mathrm{sign}b_1)\left(\frac{r_1-a_1}{2}\right)^{1/2} - \varphi\rho_f H\frac{f_c}{f}F_r\right]}{2\left[\left(\rho_{11}\rho_{22} - \rho_{12}^2 + \varphi\rho_f\rho\frac{f_c}{f}F_i\right)^2 + \left(\varphi\rho_f\rho\frac{f_c}{f}F_r\right)^2\right]},$$

$$b_2^* \equiv \frac{\varphi\rho_f\rho\frac{f_c}{f}F_r\left[R\rho_{11} + P\rho_{22} - 2Q\rho_{12} + \varphi\rho_f H\frac{f_c}{f}F_i \pm \left(\frac{r_1+a_1}{2}\right)^{1/2}\right] + \left(\rho_{11}\rho_{22} - \rho_{12}^2 + \varphi\rho_f\rho\frac{f_c}{f}F_i\right)\left[\pm(\mathrm{sign}b_1)\left(\frac{r_1-a_1}{2}\right)^{1/2} - \varphi\rho_f H\frac{f_c}{f}F_r\right]}{2\left[\left(\rho_{11}\rho_{22} - \rho_{12}^2 + \varphi\rho_f\rho\frac{f_c}{f}F_i\right)^2 + \left(\varphi\rho_f\rho\frac{f_c}{f}F_r\right)^2\right]}. \tag{13}$$

Extracting the root one more time leads to

$$V = \left(\frac{r_2^* + a_2^*}{2}\right)^{1/2} + i(\mathrm{sign}b_2^*)\left(\frac{r_2^* - a_2^*}{2}\right)^{1/2}, \tag{14}$$

where r_2^* is the modulus

$$r_2^* = \left[(a_2^*)^2 + (b_2^*)^2\right]^{1/2}. \tag{15}$$

Equation (14), combined with (1), (2), (5), (7), (13), and (15), can be used to calculate the complex velocity or the complex wavenumber for the compressional waves in an alternative way. The "minus" sign in (13) should be selected for the slow wave and "plus" for the fast wave.

The phase velocities $c = \omega/l_r$, based on Eq. (14), are calculated as

$$c = r_2^*\left(\frac{2}{r_2^* + a_2^*}\right)^{1/2}. \tag{16}$$

The use of Eq. (16) for the fast-wave calculations avoids the loss of precision at high values of porosity. However, it cannot be used for the slow-wave calculations for exactly same reason: at high porosities, r_2^* can become very close to the negative a_2^*, causing the loss of precision and instability, but this time for the slow wave. In practice, therefore, for the porosities higher than 0.85, we used Eq. (11) to compute the slow waves and Eq. (16) for the fast waves. Note that, if the porosity is smaller than approximately 0.85, either equation can be used for both types of waves.

Equations (11) and (16) are valid at all frequencies. The known high- and low-frequency phase-velocity asymptotics can be extracted from Eq. (16). The high-frequency ($f \gg f_c$) limit is obtained by dropping the terms proportional to f_c/f. This leads to $a_1 \approx (R\rho_{11} + P\rho_{22} - 2Q\rho_{12})^2 - 4(PR - Q^2)\ (\rho_{11}\rho_{22} - \rho_{12}^2)$, $b_1 \approx 0$, $r_1 \approx a_1$, $b_2^* \approx 0$, $r_2^* \approx a_2^*$, and, from Eq. (16),

$$c^2 = a_2^* = \frac{R\rho_{11} + P\rho_{22} - 2Q\rho_{12} \pm \sqrt{(R\rho_{11} + P\rho_{22} - 2Q\rho_{12})^2 - 4(PR - Q^2)(\rho_{11}\rho_{22} - \rho_{12}^2)}}{2(\rho_{11}\rho_{22} - \rho_{12}^2)}. \quad (17)$$

Equation (17) is the same as the high-frequency velocity $V_{P\infty}$ provided by Mavko et al. (2009, p. 266). What is important is that, at high frequencies, the dependence of the velocities on the structural factor δ disappears, and α remains the only free parameter through the relationships (1).

In the limit of low frequencies ($f \ll f_c$), the terms proportional to $\frac{f_c}{f}F_r$ and $\frac{f_c}{f}F_i$ become important. One needs to remember that, for the functional forms of $F(\kappa)$ considered by Biot, $F_r \to 1$ and $F_i \to 0$ as $f/f_c \to 0$ (Biot 1956b, Figs. 2 and 4). In the factor $\frac{f_c}{f}F_r$, F_r can then be replaced by unity, while the factor $\frac{f_c}{f}F_i$ is of O(1) and is much smaller. The terms proportional to $\frac{f_c}{f}F_r$ then dominate. We thus have

$$a_1 \approx -(\varphi\rho_f H\frac{f_c}{f})^2, b_1 \approx 2\varphi\rho_f\frac{f_c}{f}\left[2(PR - Q^2)\rho - H\left(R\rho_{11} + P\rho_{22} - 2Q\rho_{12} + \varphi\rho_f H\frac{f_c}{f}F_i\right)\right],$$

$|b_1| \ll |a_1|$, $r_1 \approx (\varphi\rho_f H\frac{f_c}{f})^2$ (positive, being a modulus). We also have

$$a_2^* \approx \frac{-\varphi\rho_f\rho\frac{f_c}{f}\left[\pm(\mathrm{sign}b_1)\varphi\rho_f H\frac{f_c}{f} - \varphi\rho_f H\frac{f_c}{f}\right]}{2\left(\varphi\rho_f\rho\frac{f_c}{f}\right)^2} = -\frac{H(\pm\mathrm{sign}b_1 - 1)}{2\rho} = \frac{H(1 \mp \mathrm{sign}b_1)}{2\rho} = \frac{H}{2\rho}(1 \pm 1)$$

(the minus in the final expression is for the slow wave; in the last step, an observation was made that b_1 is always negative). Further

$$b_2^* \approx \frac{\varphi\rho_f\rho\frac{f_c}{f}\left(R\rho_{11} + P\rho_{22} - 2Q\rho_{12} + \varphi\rho_f H\frac{f_c}{f}F_i\right) + \left(\rho_{11}\rho_{22} - \rho_{12}^2 + \varphi\rho_f\rho\frac{f_c}{f}F_i\right)\left[\pm(\mathrm{sign}b_1)\varphi\rho_f H\frac{f_c}{f} - \varphi\rho_f H\frac{f_c}{f}\right]}{2\left(\varphi\rho_f\rho\frac{f_c}{f}\right)^2} \approx \mp\frac{H}{2\rho}F_i,$$

where we observed that the terms proportional to $\frac{f_c}{f}F_i$ dominate over the sum of others in the parentheses (the plus in $\mp\frac{H}{2\rho}F_i$ is for the slow wave). Finally, r_2^* becomes $r_2^* \approx H/\rho$ for the fast wave and $r_2^* \approx HF_i/2\rho$ for the slow wave. Substituting the values of the coefficients into Eq. (16), we obtain the phase velocity of the fast wave as $c^2 = H/\rho$, which also is Biot's reference velocity V_c. For the slow wave, $c^2 = HF_i/\rho \approx 0$. In the low-frequency limit, therefore, only the conventional compressional wave propagates, while the slow wave disappears, as it should (cf. Biot 1956a, Figs. 3 and 5). Note that there are no free parameters in the low-frequency limit.

3. Tortuosity and its effect on wave velocities

The conclusions so far are that (1) tortuosity, as a free parameter, governs the velocities of the elastic waves at high frequencies; (2) there are no free parameters at low frequencies, and (3) both tortuosity and the structural factor affect the velocities at intermediate frequencies. We now proceed to investigating the effect of tortuosity, for which we first need to establish its physical meaning and the limits of variability.

3.1. Definitions of tortuosity

There is a lack of consistency in the literature on what should be called tortuosity. Distinct physical quantities bearing the same name have been used,

often incorrectly assumed to be interchangeable (also see Clennell 1997).

First, the "tortuosity" contained in Eqs. (1) is based on the original definitions by Biot.

Second, "tortuosity" (often denoted by T) is a parameter of the Carman-Kozeny tubular model of rock permeability. Suppose there is a tortuous tube of length L_e, and the length of a straight line connecting its ends is L, then the tortuosity in the Carman-Kozeny model is $(L/L_e)^2 \leq 1$ (Bear 1972, p. 166). To our knowledge, this purely geometric quantity has no relationship to the "tortuosity" α appearing in Eqs. (1) and controlling the dynamic coupling between the solid and the fluid in an elastic wave.

Third, Johnson et al. (1987, Eq. 2.1a) also introduce "tortuosity". It is defined for pure ideal fluid through the equation

$$\alpha\rho_f \frac{\partial \vec{U}}{\partial t} = -\nabla p, \tag{18}$$

where $\vec{U}$ is the fluid velocity and p is the pressure, which is the linearized Euler's equation with the density modified. Since this definition does not bear any relevance to the presence of the solid, α in this equation cannot be the same as α in (1) as the following demonstrates. Johnson et al. (1987, p. 392) argue that Eq. (18) can be obtained from Biot's equations of motions in the limit of stiff frame, in which they set $\vec{d} \equiv 0$ ($\vec{d}$ is the displacement of the solid) and neglect viscosity. Equation (18) then indeed follows from, for example, the second of Eqs. 3.21 and Eq. 2.3 of Biot (1956a), in which the definitions (1) are used, if $\vec{d} \equiv 0$. The latter assumption is unrealistically strong, though, as it leads to contradictions. In the same approximation, for example, the wave Eqs. (7.1) of Biot (1956a) result in $\frac{Q}{R} = \frac{\rho_{12}}{\rho_{22}}$. With the standard expressions for Q and R (Mavko et al. 2009, p. 266), $\frac{Q}{R} = \frac{1}{\varphi} - 1 - \frac{K_{fr}}{\varphi K_0}$. On the other hand, from Eqs. (1), $\frac{\rho_{12}}{\rho_{22}} = \frac{1}{\alpha} - 1$. Equating Q/R and ρ_{12}/ρ_{22} and solving for α gives $\alpha = \varphi/(1 - \frac{K_{fr}}{K_0})$. Since the stiff-frame approximation has been used, in which the deformation of the solid has been set to zero, there is no difference between the stiffnesses of the frame K_{fr} and of the pure solid K_0, both being infinitely large. Their ratio can be taken as one. The tortuosity α, therefore, will always tend to infinity, which is incompatible with Eqs. (1). Note, also, that the quantity α considered by Johnson et al. has a high-frequency limit (Johnson et al. 1987, p. 382); this contradicts the exact calculation of the tortuosity defined in Eqs. (1), which is provided in the following sections.

Still further, in Johnson et al. (1987)'s interpretation, α in Eq. (18) is a complex quantity. This also contradicts the definitions (1), from which it is necessarily real. Indeed, the quantities through which α can be expressed from (1) are the densities ρ_s and ρ_f, porosity φ, and the mass coefficients ρ_{11}, ρ_{22}, and ρ_{12} in the expression for the kinetic energy of the aggregate. All of these quantities are real-valued by their nature, therefore, α in Eqs. (1) is real-valued too.

For the rest of the article, the quantity α appearing in Eqs. (1) will be assumed when we refer to the "tortuosity".

Fourth, it is often stated that $\alpha = 1$ (the minimum possible value) for uniform cylindrical pores with axes parallel to the pressure gradient and $\alpha = 3$ for a random pore system (Mavko et al. 2009, p. 267). The latter authors refer to Stoll (1977) as the source of this result, although this publication by Stoll does not contain it. On the other hand, Stoll (1974, p. 26) does mention it, although still without a reference to the source. Clearly, the equality of α to three contradicts, for example, the definition of tortuosity cited by Bear, since that quantity cannot exceed one.

The result that α equals three for a system of randomly oriented pores, referred to by Stoll (1974) and Mavko et al. (2009), most probably dates back to Geertsma (1961, p. 236), who finally attributes the derivation to Zwikker and Kosten (1949). To see if this is a reliable foundation, we need to ascertain that the quantity discussed by Zwikker and Kosten and later by Geertsma is indeed the modern "tortuosity" in the sense of Mavko et al. (same as in Eqs. 1). In the use by Geertsma, this quantity is the "mass-coupling factor" κ (not to be confused with the argument in Biot's function $F(\kappa)$ in Eq. 2), which appears in the formula for the parameter ρ_c, $\rho_c = \kappa\rho_f/\varphi$ (Geertsma 1961, Eq. 2). By comparing Eqs. (1) of Geertsma (1961) with Eqs. (8.28) of Biot (1962b), we find that Geertsma's ρ_c is Biot's m. For m, Biot (1962b, Eqs. 8.19) has

$$m = \rho_{22}/\varphi^2. \tag{19}$$

Equating ρ_c and m then leads to $\rho_{22} = \varphi\rho_f$, which coincides with ρ_{22} from Eqs. (1) and shows that Geertsma's κ is indeed the tortuosity α. Now, in turn, we need to make sure that the parameter used by Zwikker and Kosten, referred to by Geertsma, still has the same meaning. Zwikker and Kosten (1949, Eq. 1.23) call it the "structure constant" k, which is postulated to appear in the non-viscous equation of motion for the air enclosed in a pore, $\frac{k}{\varphi}\rho_f\frac{\partial U}{\partial t} = -\frac{\partial p}{\partial x}$. This equation contradicts in form Eq. (18) used by Johnson et al. (1987), demonstrating that there is not a unique way to formulate such a relation. In our view, both are inaccurate, because they both deviate from Euler's equation, one of the main equations of fluid mechanics. Further, even if Eq. (18) were correct, Zwikker and Kosten's "structure constant" k would still not be the quantity identical with α. This is one reason why Zwikker and Kosten's inferred behavior of k does not apply to the possible behavior of the tortuosity. Another reason is that Zwikker and Kosten's conclusions do not seem to be well founded either. The authors' inference that the structural factor for a system of randomly oriented pores equals three appears to follow from their averaging the factor $1/\cos^2\theta$, where θ is the angle between the pore axis and the direction of the pressure gradient (Zwikker and Kosten 1949, p. 21). The origin of this conclusion is unclear, because averaging this factor over all possible angles would involve the diverging integral $\int_0^\pi d\theta/\cos^2\theta$.

We conclude that the inference about the tortuosity ranging from one to three between the system of pores oriented in the direction of pressure gradient and the system of random pores does not appear to be well founded. This inference also implies that the tortuosity is constant for any given pore geometry, whereas, as we will see next, it exhibits, even for the simplest cases, a complex frequency dependence.

3.2. *Exact calculation of tortuosity*

We see that the meaning of the tortuosity has been far from being clear. The nature of this parameter can be best understood from its definition. The quantity α originates in the coupling coefficients ρ_{11}, ρ_{12}, ρ_{22} (Eqs. 1), which were introduced by Biot in the expression for the kinetic energy of the fluid–solid aggregate (Biot 1956a, Eq. 3.2). Molotkov (2002), based on this definition of ρ_{11}, ρ_{12}, and ρ_{22}, derived relations (1) and the exact formula for the parameter α. It is useful for the characterization of the behavior of α to consider a simple example, in which the tortuosity can be calculated exactly. We consider a simple example of a one-dimensional fluid-filled conduit bounded by two parallel solid surfaces, corresponding to Biot's "slit-type" pore (Biot 1956b, Fig. 1, reproduced in Fig. 1 here). The solid walls are oscillating along their boundaries. For this case,

$$\alpha = 1 + \frac{\int_{-a}^{a}(U-\bar{U})^2 dy}{2a(\bar{U}-\bar{u})^2}, \tag{20}$$

where U and u are the velocities of the fluid and the solid in the direction of the pore axis, respectively; the integration is performed over the width $2a$ of the pore in the direction y perpendicular to the axis, and the overbar means the average over the pore width (Molotkov 2002, Eqs. 11, 12). Note that Molotkov's article contains a typo: it shows a factor of two before the second term in Eq. (20), while it should be one.

Note that Biot (1962b, Eqs. 8.19) introduced the parameter m that is equivalent to the tortuosity; however, Biot did not provide any clear means to calculate it. Equation (20) fills this gap.

In calculating the exact tortuosity for this simple system, we can make use of the results already available from the work by Biot. Biot (1956b) worked with the relative velocity of the fluid, $U_1 = U - u$. Replacing U in Eq. (20) with $U = U_1 + u$, we obtain $\alpha = 1 + \frac{\int_{-a}^{a}[(U_1-\bar{U}_1)+(u-\bar{u})]^2 dy}{2a\bar{U}_1^2} = 1 + \frac{\int_{-a}^{a}[(U_1-\bar{U}_1)]^2 dy}{2a\bar{U}_1^2}$, where, in

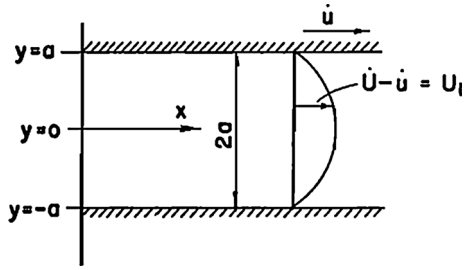

Figure 1
Biot's slit pore (after Biot 1956b, Fig. 1)

the last step, we used the fact that the velocity at any given time is the same on the solid walls, $u = \bar{u}$. Then, in completing the square of the bracketed expression and noting that $\frac{1}{2a}\int_{-a}^{a} U_1 dy = \bar{U}_1$, we obtain

$$\alpha = \frac{\int_{-a}^{a} U_1^2 dy}{2a\bar{U}_1^2}, \tag{21}$$

which can be recast as

$$\alpha = \overline{U_1^2}/\bar{U}_1^2. \tag{22}$$

The tortuosity then acquires a particularly transparent physical meaning being the normalized average square of the relative velocity of the fluid. Equation (22) for the tortuosity was previously given by Allard and Atalla (2009, Eq. 5.21) without derivation; α was assumed to be frequency-independent. We will next see that the exact calculation using Eq. (22) shows that this is not the case. Allard and Atalla (2009) also overlook the fact that the relative velocity U_1 should enter Eq. (22), which becomes important when the pore walls are moved by an elastic wave.

We note that, similar to Eqs. (1), Eq. (22) also precludes α from being a complex quantity. The velocity U_1 is a physical field, for which only the real component carries physical meaning. As is well known, representing a physical field as a complex quantity (such as in Eq. 23) provides convenience in the mathematical manipulations on the field as long as only the linear operations are performed (e.g., Landau and Lifshitz 1959, p. 89). Equation (22) represents the tortuosity through a nonlinear operator on U_1 and, therefore, has to use the real part of U_1 to avoid meaningless results.

In Eq. (21), U_1 and $\bar{U}_1$ are the instant real-valued velocities. On the other hand, assuming a sinusoidal time dependence, Biot deals with the complex velocities,

$$U_1 \equiv U_{10}e^{i\omega t}, \quad \bar{U}_1 \equiv \bar{U}_{10}e^{i\omega t}. \tag{23}$$

For the slit model, he provides the analytical expressions for the complex amplitudes U_{10} and $\bar{U}_{10}$:

$$U_{10} = \frac{X_0}{i\omega}\left\{1 - \frac{\cosh\left[\left(\frac{i\omega}{\nu}\right)^{1/2} y\right]}{\cosh\left[\left(\frac{i\omega}{\nu}\right)^{1/2} a\right]}\right\}, \tag{24}$$

$$\bar{U}_{10} = \frac{X_0}{i\omega}\left\{1 - \frac{1}{a}\left(\frac{\nu}{i\omega}\right)^{1/2}\tanh\left[\left(\frac{i\omega}{\nu}\right)^{1/2} a\right]\right\}, \tag{25}$$

where $\nu = \eta/\rho_f$, and η is the viscosity of the fluid (Biot 1956b, Eqs. 2.9 and 2.11, respectively). (To emphasize that a quantity is a complex amplitude, we have added a subscript "zero" to it, while Biot drops it). In writing Eqs. (24) and (25), X in the body force $X\rho_f = -\frac{\partial p}{\partial x} - \rho_f \ddot{u}$ (Biot 1956b, Eq. 2.4) was represented as

$$X = -\frac{1}{\rho_f}\frac{\partial p}{\partial x} - \ddot{u} \equiv X_0 e^{i\omega t}, \tag{26}$$

where X_0 is a complex amplitude. For the instant velocity, keeping in mind (23) and (26), Eq. (24) can be re-written as

$$U_1 = \frac{X}{i\omega}\left\{1 - \frac{\cosh\left[\left(\frac{i\omega}{\nu}\right)^{1/2} y\right]}{\cosh\left[\left(\frac{i\omega}{\nu}\right)^{1/2} a\right]}\right\}. \tag{27}$$

We can us assume that $X = -\frac{1}{\rho_f}\frac{\partial p}{\partial x} - \ddot{u}$ is a real-valued external forcing on the fluid (it can be checked that it can always be represented as $X_0 e^{i\omega t}$). From (27), we then obtain the real-valued instant velocity,

$$\mathrm{Re}(U_1) = -\frac{X}{\omega}\frac{\cos(\gamma y)\cosh(\gamma y)[\tan(\gamma y)\tanh(\gamma y) - \tan(\gamma a)\tanh(\gamma a)]}{\cos(\gamma a)\cosh(\gamma a)\left[1 + \tan^2(\gamma a)\tanh^2(\gamma a)\right]}, \tag{28}$$

where we have introduced the notation $\gamma \equiv (\omega/2\nu)^{1/2}$.

Likewise, from (25), using (23) and (26), we obtain

$$\mathrm{Re}(\bar{U}_1) = \frac{X}{4a\gamma\omega}\frac{\sin(2\gamma a) - \sinh(2\gamma a)}{\cos^2(\gamma a)\cosh^2(\gamma a)\left[1 + \tan^2(\gamma a)\tanh^2(\gamma a)\right]}. \tag{29}$$

The tortuosity α is then calculated from Eq. (21) as $\alpha = \frac{\int_{-a}^{a}[\mathrm{Re}(U_1)]^2 dy}{2a[\mathrm{Re}(\bar{U}_1)]^2}$ by substituting Eqs. (28) and (29). After completing the integral, we arrive at

$$\alpha = \frac{\gamma a \cos^2(\gamma a)\cosh^2(\gamma a)}{[\sin(2\gamma a) - \sinh(2\gamma a]^2} \times \Big\{ 4\gamma a\left(p^2-1\right) + 2[\sin(2\gamma a) + \sinh(2\gamma a)]\left(p^2+1\right) + \sin(2\gamma a)\cosh(2\gamma a)\left[2p^2 - (p+1)^2\right] + \sinh(2\gamma a)\cos(2\gamma a)\left[2p^2 - (p-1)^2\right] \Big\}, \tag{30}$$

where, for brevity, we introduced the notation $p \equiv \tan(\gamma a)\tanh(\gamma a)$. Notice that the form of the term X does not eventually matter as it cancels in the calculation of α. Also note that α is a function of a single parameter $\gamma a = \left[\frac{f}{v/(\pi a^2)}\right]^{1/2}$. Using Eqs. (4.8) and (4.24) of Biot (1956b), for the slit pore we obtain

$$f_c = 3v/(2\pi a^2). \tag{31}$$

The parameter γa, therefore, can be cast in terms of the characteristic frequency,

$$\gamma a = \left(\frac{3}{2}\frac{f}{f_c}\right)^{1/2}. \tag{32}$$

The tortuosity α is then a function of f/f_c only.

3.3. Properties of tortuosity

3.3.1 The range of change in f/f_c

For the slit-like pore, the characteristic frequency is given by Eq. (31); for the cylindrical pore, it is given by $f_c = 4v/(\pi a^2)$ (Biot 1956b, Eq. 4.15). In both cases, f_c has the order of v/a^2. In a typical porous rock, pore widths range approximately from 10^{-6} to 10^{-4} m. Take the representative values of $\eta = 10^{-3}$ Pa $\times$ s and $\rho_f = 10^3$ kg/m^3, then f_c ranges from 10^2 to 10^6 Hz. Frequencies as low as 10 Hz are important for seismic exploration, and frequencies as high as 10^7 Hz are used in laboratory studies of acoustic properties of rocks. The overall expected range of change in the dimensionless frequency f/f_c, of interest to rock-physics applications, therefore, is approximately 10^{-5}–10^5.

3.3.2 Dependence of tortuosity on f/f_c

Figure 2 plots α calculated from Eq. (30) as a function of f/f_c, using the relation (32) in the argument. Several observations regarding the properties of the tortuosity can be made.

First, there is an opinion in the literature that the tortuosity α is a purely geometric factor (e.g., Mavko et al. 2009, p. 267). The theoretical tortuosity plotted in Fig. 2 shows that this is not the case: α exhibits a strong frequency dependence. This dependence was anticipated by Biot. On p. 1495 of Biot (1962b), one reads, "Strictly speaking, a (frequency) correction must apply to the density parameters ρ_{11}, ρ_{12}, and ρ_{22} to take into account the departure of the microvelocity field from Poiseuille flow as the frequency increases." This is exactly what Eq. (30) accomplishes.

At frequencies satisfying the condition $f/f_c \lesssim 1$, the flow is of Poiseuillean type (cf. Biot 1956a, Eq. 6.11). The tortuosity in this range changes from its asymptotic value of 6/5 to a local minimum of almost exactly one. At these frequencies, the channel width becomes comparable to or is smaller than the viscous skin depth $\left(\frac{v}{\pi f}\right)^{1/2}$, or the effective depth of penetration of the oscillatory motion of the wall (Landau and Lifshitz 1959, Eq. 24.5). In the Poiseuillean flow regime, the entire fluid profile across the channel moves in phase, explaining the simple behavior of the tortuosity.

At higher frequencies, the flow is no longer Poiseuillean and α is no longer constant. Instead, it infinitely grows as frequency increases. In this flow regime, part of the fluid profile near the wall, within

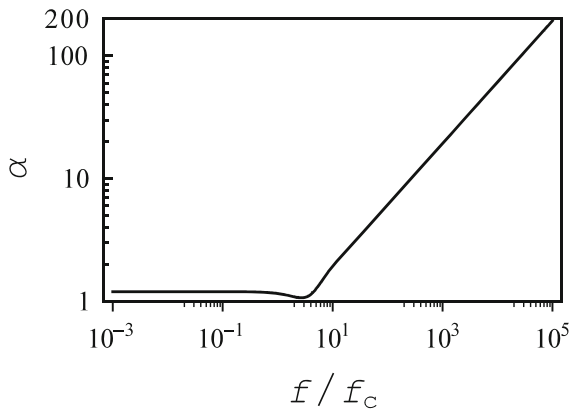

Figure 2
Tortuosity for the slit-like pore as a function of dimensionless frequency

the skin-depth boundary layer, moves out-of-phase with the rest of the channel, explaining the more complex, frequency-dependent, behavior of the tortuosity. The high-frequency ($\gamma a \gg 1$) asymptotics of α is $\alpha = \gamma a/2$. It can be obtained from Eq. (30) by using the properties of the hyperbolic functions at large argument: $\tan x \to 1$; $\sinh x, \cosh x \gg \sin x, \cos x$, and $\sinh x \approx \cosh x \approx e^x/2$, all as $x \to \infty$. From Eq. (32), the asymptotics is then $\alpha = \left(\frac{3}{8}\frac{f}{f_c}\right)^{1/2}$, representing a straight line on the log–log scale having f/f_c as the abscissa. This is the equation of the straight line seen at high frequencies in Fig. 2; α follows the asymptotic equation almost exactly already at $f/f_c \gtrsim 6$.

Second, the practical range of change in α, based on this simple model, is between approximately 1 and 100.

Biot (1962a, p. 1258) states without derivation that the parameter m for the slit varies from $(6/5)\rho_f$ to ρ_f over the entire frequency range. To put this result into our context, we substitute the second of Eqs. (1) into (19), arriving at $\alpha = \frac{m\varphi}{\rho_f}$. The range of change in m found by Biot then leads to the range in α from $(6/5)\varphi$ to φ. This result is exactly the low-frequency behavior of α seen in Fig. 2 if in the last equation we formally set $\varphi = 1$ for the slit (the latter will no longer be correct if we assume a finite thickness of the wall, whereas Eq. 30 will still be valid). The conclusion by Biot also does not capture the square-root increase in α at higher frequencies.

Figure 2 shows that, even for the simplest case of a slit-like pore, the tortuosity exhibits a complex behavior. Figure 2 was obtained for the case of one-dimensional wave propagation with the oscillations of both solid and the fluid in the plane of the solid wall. However, in the definition of the coefficients ρ_{11}, ρ_{12}, ρ_{22}, Biot does not make a distinction between those defined for the one-dimensional case and those for the general three-dimensional propagation (cf. Eqs. 3.2 and 3.3 of Biot 1956a). The lack of such a distinction is indeed justified for the isotropic scenario considered by Biot, in which there is no preferred particle-velocity direction. Equation (22) hence is still valid (also see Molotkov 2002, Eqs. 20). In cases of complex geometries, calculation of the tortuosity will require the knowledge of the fluid-velocity field, which cannot be obtained analytically but for the simple one-dimensional ducts and tubes, and can be calculated numerically for somewhat more involved cases. For one-dimensional channels, because of the symmetry, the velocity field and, hence, the tortuosity do not depend on which direction the fluid is flowing, as exemplified by Eq. (30). In three-dimensional porous geometries with no symmetries, the flow field will depend on the direction of the driving body force; the latter, as in Eq. (26), will generally include the components from the pressure gradient and the inertial forcing caused by the wave-induced acceleration of the wall. In the absence of symmetries, the tortuosity, therefore, can be expected to depend on both the direction of the gradient and the wave-propagation direction. In the general case of wave propagation in porous rocks with irregular pore structure of unknown complexity, the fluid-velocity field, and hence the tortuosity, are unpredictable.

The conclusion is that the behavior of α in realistic porous structures can be even more complex, in unknown ways, than that exhibited in Fig. 2, and is generally unpredictable.

3.4. *Effect of tortuosity on wave velocities*

Having established the general properties of the tortuosity, for the simple case allowing analytical treatment, we can investigate the effect of this parameter on the propagation of the fast and slow waves.

To use expressions (11) or (16) for the phase velocities, we need the explicit relations for the real and imaginary parts of Biot's correction function $F(\kappa)$. For the slit-like pore model under consideration, $F(\kappa)$ is

$$F(\kappa) = \frac{1}{3}\frac{i^{1/2}\kappa \tanh(i^{1/2}\kappa)}{1 - \frac{1}{i^{1/2}\kappa}\tanh(i^{1/2}\kappa)} \tag{33}$$

(Biot 1956b, Eq. 2.17). Extracting the real and imaginary parts of Eq. (33) leads to

$$F_r(\kappa) = \frac{\sqrt{2}}{3}\kappa^2 \frac{-\sin(\sqrt{2}\kappa)\{\kappa[\cosh(\sqrt{2}\kappa)+\cos(\sqrt{2}\kappa)] - \sqrt{2}\sinh(\sqrt{2}\kappa)\} + \sinh(\sqrt{2}\kappa)\{\kappa[\cosh(\sqrt{2}\kappa)+\cos(\sqrt{2}\kappa)] - \sqrt{2}\sin(\sqrt{2}\kappa)\}}{\{\kappa[\cosh(\sqrt{2}\kappa)+\cos(\sqrt{2}\kappa)] - \sqrt{2}\sinh(\sqrt{2}\kappa)\}^2 + \{\kappa[\cosh(\sqrt{2}\kappa)+\cos(\sqrt{2}\kappa)] - \sqrt{2}\sin(\sqrt{2}\kappa)\}^2},$$

$$F_i(\kappa) = \frac{\sqrt{2}}{3}\kappa^2 \frac{\sinh(\sqrt{2}\kappa)\{\kappa[\cosh(\sqrt{2}\kappa)+\cos(\sqrt{2}\kappa)] - \sqrt{2}\sinh(\sqrt{2}\kappa)\} + \sin(\sqrt{2}\kappa)\{\kappa[\cosh(\sqrt{2}\kappa)+\cos(\sqrt{2}\kappa)] - \sqrt{2}\sin(\sqrt{2}\kappa)\}}{\{\kappa[\cosh(\sqrt{2}\kappa)+\cos(\sqrt{2}\kappa)] - \sqrt{2}\sinh(\sqrt{2}\kappa)\}^2 + \{\kappa[\cosh(\sqrt{2}\kappa)+\cos(\sqrt{2}\kappa)] - \sqrt{2}\sin(\sqrt{2}\kappa)\}^2}. \quad (34)$$

In calculating the wave velocities, the argument of $F(\kappa)$ as in Eq. (2) will be used.

Figure 3 presents the frequency dependences of the fast (a) and slow (b) wave velocities for the two end values of the parameter α, $\alpha = 1$ and $\alpha = 100$, representing the range of change established from the analysis of the slit-like model. The velocities have been normalized by the reference velocity V_c. The calculations were performed using Eq. (11), combined with (1), (5), (7), (8), (10), and (34). The porosity is $\varphi = 0.5$. The constants P, Q, and R were calculated through the formulae given by Mavko et al. (2009, p. 266) (which are equivalent to Eqs. 21 and 24 of Biot and Willis 1957), with $K_0 = 37$ GPa (bulk modulus of pure quartz) and $K_f = 2.25$ GPa (bulk modulus of water). To determine K_{fr} and μ_{fr}, we applied an empirical relation developed by Krief et al. (1990) used for velocity-porosity model calibrations (e.g., Goldberg and Gurevich 1998): $K_{fr} = (1-\varphi)^{\frac{3}{1-\varphi}}K_0$, $\mu_{fr} = (1-\varphi)^{\frac{3}{1-\varphi}}\mu$, where μ is the shear modulus of the pure solid. For μ and ρ_s, we took the values for quartz, $\mu = 45$ GPa and $\rho_s = 2650$ kg/m^3, and, for ρ_f, the value for water, $\rho_f = 997$ kg/m^3. Finally, for the parameter δ, we took $\delta = \sqrt{16/3}$, which is the minimum value used by Biot (1956b, Eqs. 4.31–4.34). We remind, though, that Biot's assignment of a number to δ had arbitrary character; we will devote a more detailed discussion to the effect of this uncertainty in a later section.

From Fig. 3a, b, we see that the general effect of increasing α is to lower the velocities of both the fast and the slow waves. However, the effect is much stronger for the slow wave. To illustrate, Fig. 3c shows the ratio of the velocities at two end values of α, $c(\alpha = 1)/c(\alpha = 100)$, for both waves. The respective change in the slow-wave speed is over an order

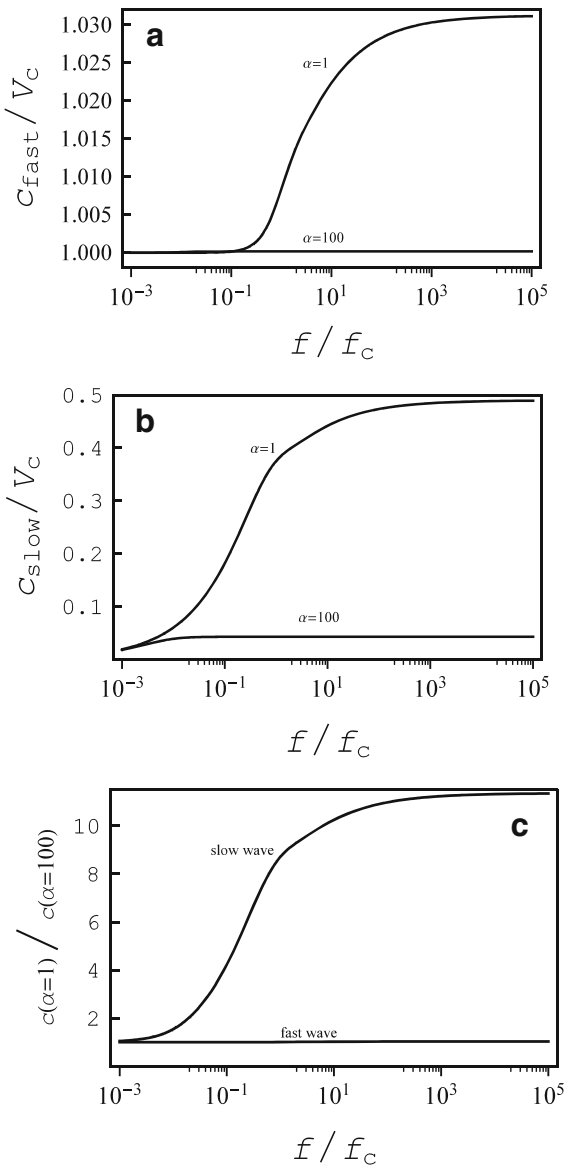

Figure 3
Effect of tortuosity on wave velocities. $\varphi = 0.5$ and $\delta = \sqrt{16/3}$

of magnitude, whereas the change in the fast-wave speed is only approximately 3 percent and is not even seen on the scale of the graph in Fig. 3c.

Figure 4 shows the same frequency dependences of the wave speeds at an increased value of porosity, $\varphi = 0.8$. As we explained earlier, the calculations for the slow wave were performed in the same way (through Eq. 11) as for Fig. 3; for the fast wave, we used Eq. (16). Everything else is the same as for Fig. 3. The conclusions regarding the sensitivity of the fast- and slow-wave speeds to the parameter α, drawn from Fig. 4, remain the same as for Fig. 3, except that the increasing porosity virtually eliminates the realistic existence of the slow wave, whose speed vanishes.

We infer that, for all practical purposes, the effect of the tortuosity can be neglected at all frequencies, low and high, for the conventional compressional wave, for which α does not serve as a significant governing parameter. The effect of α is only of interest as far as the slow wave (the wave of the second kind) is concerned.

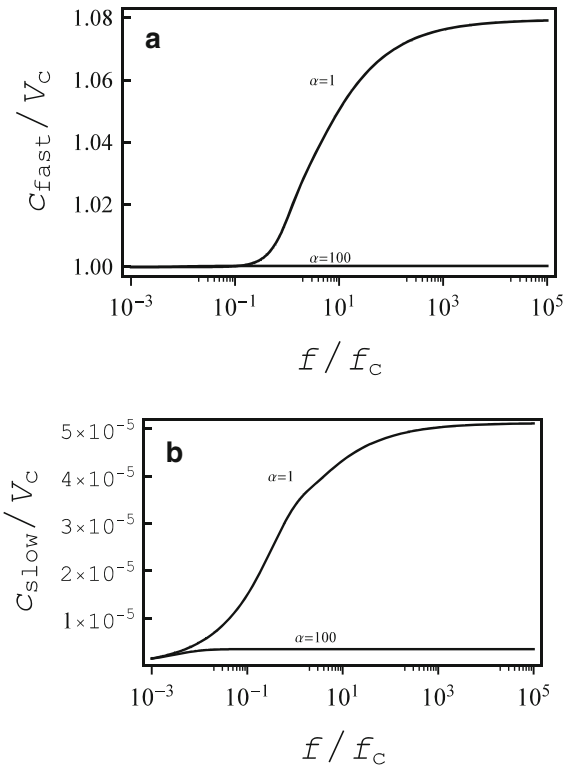

Figure 4
Effect of tortuosity on wave velocities. $\varphi = 0.8$ and $\delta = \sqrt{16/3}$

An important conclusion is also made. We have earlier established that the behavior of the tortuosity α for any realistic porous structure can be supposed to be unpredictably complex. On the other hand, the speed of the wave of the second kind, based on Biot's theory, depends significantly on this parameter. We conclude that the properties of the wave of the second kind are unpredictable for any practical situation, which is an inherent limitation in the applications of Biot's theory.

3.5. *Other theoretical calculations of tortuosity*

There were attempts in the past to theoretically calculate the tortuosity (or the equivalent coefficients ρ_{11}, ρ_{12}, and ρ_{22} in Eq. 1). Hovem and Ingram (1979, Eq. 8) theoretically derived an expression for ρ_{12}. Their simple equations of motion (Hovem and Ingram 1979, Eqs. 6) only include a phenomenologically defined friction force and do not contain a driving force; in spite of this, a sinusoidally varying solution is assumed. This is incorrect, because an equation with damping and without a driving force cannot support a sinusoidal solution. As a result, a contradiction is obtained. Specifically, Hovem and Ingram obtain ρ_{12} by cross-comparing the coefficients in their re-written equations of motions (7) with the coefficients in the respective terms of Eqs. (6.5) of Biot (1956a). Although the authors only deduce ρ_{12} from this comparison, the coefficients ρ_{11} and ρ_{22} can be obtained as well. For example, the comparison implies that $\rho_{11} = \rho_s - \rho_{12}$ and $\rho_{22} = \rho_f - \rho_{12}$, which are not the correct properties of the coefficients in Eqs. (1).

Bedford et al. (1984) propose a different method of calculating ρ_{12} from the original Biot equations. They substitute the solutions in the form $u = e^{i\omega t}$ and $U = U_0 e^{i\omega t}$ directly into one of Biot's equations of motion for the aggregate (Bedford et al.'s Eq. 2, which is equivalent to the second of Eqs. 6.7 of Biot 1956a). The result is solved for ρ_{12} as a function of the complex amplitude U_0 (Bedford et al. 1984, Eq. 7) (ρ_{12} is $-c$ in Bedford et al.'s notation). The authors then substitute the known solutions of the Navier–Stokes equations for U_0 for one-dimensional cylindrical geometries into their expression for ρ_{12}, resulting in a frequency-dependent behavior of this

coefficient (Bedford et al. 1984, Fig. 8). We note that this algorithm of finding ρ_{12} is flawed, too, because the solutions of the Navier–Stokes equations are not necessarily the solutions of the Biot equations. As a result, Bedford et al.'s approach leads to a paradox as well. Biot (1956a, Eqs. 6.7) has two coupled equations of motion for the aggregate, each containing ρ_{12}. Bedford et al. resolved ρ_{12} from the second of these equations. We observe that an expression for ρ_{12} can also be obtained from the first of Biot's equations (equivalent to Bedford et al.'s Eq. 1). The resulting expressions for ρ_{12} must be equal. Equating them and solving the result for U_0 leads to $U_0 = \frac{(\varphi-1)\rho_s}{\varphi\rho_f}$. The latter result is paradoxical, since it means that U_0 is constant and independent of frequency, which contradicts the original solution of the Navier–Stokes equation used (Eq. 11 of Bedford et al.) and the authors' prior conclusion that ρ_{12} was frequency-dependent (Bedford et al. 1984, Fig. 8). Formally speaking, this paradox demonstrates that the phenomenological Biot equations are incompatible with the Navier–Stokes equations.

3.6. *Measurements of tortuosity*

Is tortuosity truly a free parameter, or can it be measured? Measurements of α have also been proposed.

Brown (1980), based off of a vague analogy between the flow of ideal fluid and electrical-current flow, obtained the difference between what he calls the "apparent and actual" fluid densities, which he arbitrarily equates to Biot's "additional mass" ρ_a, $\rho_a = \rho_f(\lambda - 1)$, where λ is Brown's "coupling coefficient", $\lambda = F\varphi$, and F is the electrical-resistivity formation factor (the ratio between the aggregate and the fluid resistivities) (Brown 1980, Eqs. 7, 8). From one of Biot's relations (Biot 1956a, Eqs. 3.18), this means that $\rho_{12} = -\rho_a = \rho_f(1 - \lambda)$, and ρ_{12} thus could be measured by electrical means. Brown (1980, p. 1269) also claims that this result is valid for high frequencies. For the given fluid density, porosity, and electrical properties, the high-frequency ρ_{12} (and, therefore, α) are, therefore, constant and independent of frequency, which is in conflict with the theoretical calculation of α showing no high-frequency limit (Eq. 30 and Fig. 2). Note that Johnson et al. (1987, Eq. 2.8) use Brown's result to support the existence of the high-frequency limit of the tortuosity α. Further, Johnson et al. (1982, p. 1841), followed by Zhou and Sheng (1989, Eq. 27), directly equate Brown's high-frequency coupling coefficient λ with α. This is incorrect. Equating Brown's ρ_{12} with ρ_{12} from Eq. (1), $\rho_f(1 - \lambda) = (1 - \alpha)\varphi\rho_f$, yields $\lambda = 1 - (1 - \alpha)\varphi$, which is not the same as $\lambda = \alpha$.

The dynamic-permeability model developed by Zhou and Sheng (1989), therefore, also treats the tortuosity as a constant quantity at high frequencies. The authors report its numerical values ranging from 1 to 24 for three periodic models of porous media (Zhou and Sheng 1989, p. 12034 and Table 1), although no details are given as to what specific formulae for the tortuosity were used to calculate those values.

Johnson (1980) proposed to determine the tortuosity from the measured speed C_4 of the fourth sound in superfluid ^{4}He at low temperatures. The relation between the experimentally determined value C_4^E in a superfluid-filled porous solid and the theoretical speed C_4^0 in the pure superfluid is $C_4^E = C_4^0/n$, where n is the "index of refraction" (Johnson 1980, Eq. 5). On the other hand, in the stiff-frame limit ($K_f \ll K_{fr}$, μ_{fr}), the equation for the phase velocity of Biot's slow-wave at high frequencies (Eq. 17 with the negative sign at the root) reduces to $c_{slow} = (K_f/\alpha\rho_f)^{1/2} = c_f/\alpha^{1/2}$, where c_f is the sound velocity in the pure fluid. Based on the analogy between the two expressions, Johnson (1980) argues that the fourth sound in the superfluid is Biot's slow wave, therefore, $n = \sqrt{\alpha}$, and α can thereby be measured in acoustic experiments on porous samples filled with liquid ^{4}He. We make two observations in regard of this argument. First, the similarity between the two expressions does not guarantee that they describe the same physical phenomenon, unless the fourth sound in a porous solid is governed by the Biot equations. The latter has not been shown. Second, n is a purely geometrical quantity (Johnson 1980, p. 1066), and the high-frequency measurements in liquid helium will yield a constant value. This is again in conflict with the exact calculation of α, based on its original definition, which shows strong frequency dependence (Fig. 2).

Johnson et al. (1994a, b) report successful experimental verification of the theoretical predictions of

the speed and attenuation of the fast and slow waves based on their measurement of tortuosity. One should remember, though, that an additional free parameter (Λ in their original notation) was specifically fit to match the data (Johnson et al. 1994, pp. 109–110).

4. *Structural factor and its effect on wave velocities*

We now investigate the effect of the structural factor on the propagation of the fast and slow waves. As we have established, the effect can be expected at intermediate frequencies.

Unlike tortuosity, the structural factor has no particular physical meaning, except quantifying the geometrical properties of the porous space in largely unknown ways. Biot (1956b, Eqs. 4.31–4.34) speculated that δ may range from $\sqrt{16/3}$ to $\sqrt{8\times\frac{3}{2}}$, although the choice of this interval had no particular justification. It should be noted that another quantity has been frequently invoked in the literature as a substitute for Biot's δ. Biot's theoretical expressions for the frequency parameter κ in Eq. (2) for the slit- and tube-like pores have the form $\kappa = a(\omega/v)^{1/2}$, where a is a characteristic pore width (Biot 1956b, Eqs. 2.14, 3.11). It has been proposed that the quantity a, named the "pore-size factor", be considered the free geometric parameter (Stoll 1974, p.27; Mavko et al. 2009, p. 269). As comparison with Eq. (2) shows, both a and δ have the same effect on κ, being scaling factors before the square root of the frequency. In the following, we will keep Biot's original structural parameter δ as the measure of the geometric complexity of the porous space. In the absence of the theoretical constraints on its values for complex geometries, δ (or a) became mere formal fitting parameters.

Figure 5 presents the frequency dependences of the fast (a) and slow (b) wave velocities for two end values of δ, $\delta = \sqrt{16/3}$ and a factor-of-fifty greater value $\delta = 50\sqrt{16/3}$. As already noted, there is significant uncertainty in ascertaining the actual range in which δ can change. The low value was selected as the minimum one used by Biot. Regarding the high value, we note that the pore-size parameters a found by Stoll (1974, Table 1) by fitting experimental data vary by a factor of 515, and those found by Gurevich et al. (1999, Table 1) by a factor of 46. We consider the variability reported by Stoll to be rather extreme and, for the illustrative purposes, chose to use the range obtained by Gurevich et al., as it was determined by simulating the data from much more recent and well established experiments. We will make more comments on the variability of the structural factor further in this section.

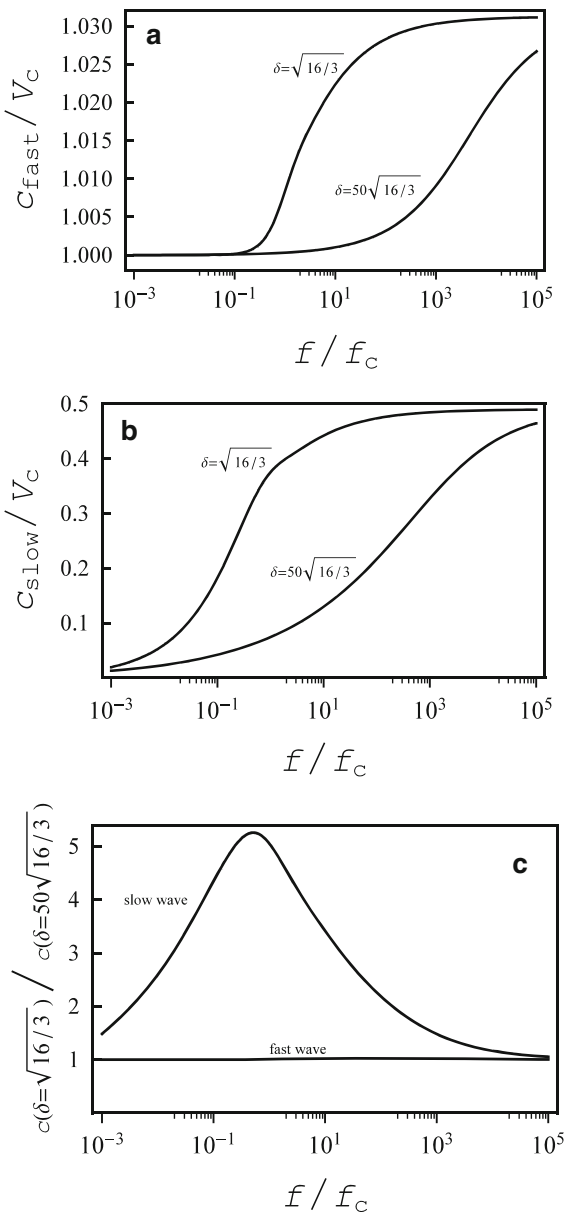

Figure 5
Effect of structural factor on wave velocities. $\varphi = 0.5$ and $\alpha = 1$

In Fig. 5, the tortuosity was fixed at $\alpha = 1$, representative of the most used literature values, and $\varphi = 0.5$. The elastic constants are the same as in Figs. 3 and 4. The calculations were performed through Eq. (11). As Fig. 5 demonstrates, the structural factor affects the wave speeds at intermediate frequencies only as anticipated. The effect of increasing δ is similar to that of increasing α (cf. Figs 3 and 5): the velocities of both the wave of the first and the second kind become lower, and the effect on the slow wave is by far stronger. The sensitivity to the change in the parameter δ across its full range is illustrated in Fig. 5c, which plots $c(\delta = \sqrt{16/3})/c(\delta = 50\sqrt{16/3})$ for both waves. The fast wave is largely insensitive to the change in the structural parameter (its speed varies by about 3 percent), while the slow-wave speed varies by about a factor of five. What is important is that the effect of α, across its full range, on the slow-wave speed is still a factor of two stronger in the same frequency band (cf. Figs 3c and 5c). We thus infer that the influence of δ overall is insignificant compared with the respective effect of α, at all frequencies. The conclusion is that the structural factor is not a significant free parameter of Biot's theory and can practically be ignored, its effect being dwarfed by that of the tortuosity. The tortuosity α becomes the only free parameter of the theory, and it is only important for the calculation of the slow waves at high frequencies.

As noted in this section, a large variability of the pore-size factor up to two orders of magnitude was reported by Stoll (1974, Table 1) and Gurevich et al. (1999, Table 1). In fitting the parameter a, both studies fixed the tortuosity α at constant values. The experimental data simulated by Gurevich et al. and part of the data fitted by Stoll were in the MHz frequency range. Considering our estimated range of change in the characteristic frequency f_c from approximately 10^2 to 10^6 Hz, it is most likely that the simulated data lay in the "high-frequency" range of Biot's theory where the effect of the pore-size factor is negligible compared to the effect of α. Fitting the data letting a be free while fixing α could then produce an artificially large variation of the former, given that it had to change substantially to have any pronounced influence on the simulated waves. A parameter trade-off may have occurred, which needs to be taken into account in interpreting the significance of the wide range of the pore-size factor reported.

Also, as Eq. (33) shows, we chose a particular form of Biot's correction function $F(\kappa)$ derived for the slit duct. The close quantitative similarity between the functions $F(\kappa)$ obtained by Biot for the cylindrical tube and the slit (cf. Biot 1956b, Figs. 2 and 4) supports a hypothesis that their form may remain similar for more complex geometries, although this is not guaranteed. This imparts an additional source of uncertainty to the simulations of the effect of the structural factor, which was not investigated here.

5. Conclusions

Our conclusions can be formulated as follows.

The tortuosity α is the only significant free parameter of Biot's theory, whose effect is limited to the waves of the second kind in the high-frequency range. The conventional compressional wave (wave of the first kind) is largely insensitive to the changes in tortuosity at any frequencies. The structural factor δ affects the wave properties at intermediate frequencies only and, even in that interval, its effect is practically dwarfed by the one of the tortuosity. The effect of δ can thus be neglected in practical calculations.

At low frequencies, there are no free parameters. The wave of the second kind is virtually non-existent (its speed vanishes). Considering that the frequency band of interest to seismic exploration is approximately 10–10^2 Hz and that the change in the characteristic frequency for rocks is estimated as 10^2–10^6 Hz, the "seismic" range in f/f_c is approximately 10^{-5}–1; that is, the "seismic" case is largely immune to the uncertainties in the theory that may be associated with the lack of constraints on its free parameters.

The tortuosity has the meaning of the mean square of the velocity of the pore fluid relative to the pore wall, normalized by the square of the mean relative velocity. Its exact calculation requires the knowledge of the full fluid-velocity field. Analytical calculation of α is possible for the model of a slit-like pore considered by Biot but not for more geometrically complex situations. For the latter, numerical calculation of α may be possible, as long as the flow field can be computed. The tortuosity for the slit is

constant at the values close to unity at $f/f_c \lesssim 1$, where flow is of Poiseuillean type, and rises infinitely at higher frequencies, where the flow changes phase across the width of the channel. It thus has no high-frequency limit. The practical range of variability in α, inferred from this model, is approximately 1–100.

The functional form of the tortuosity for more complex geometries is unknown and can be hypothesized to be unpredictably complex for realistic earth materials. Since the properties of the wave of the second kind depend substantially on this parameter at high frequencies, they cannot be predicted by the theory for any realistic situation. This is an inherent limitation of the Biot theory, restricting its usefulness for the prediction of wave propagation in the high-frequency range.

Acknowledgments

Constructive reviewer comments are appreciated.

References

Abramowitz, M., & Stegun, I. A. (Eds.) (1964). Handbook of mathematical functions: National Bureau of Standards, Washington, D.C.

Allard, J. F., & Atalla, N. (2009). Propagation of sound in porous media: Wiley.

Bear, J. (1972). Dynamics of fluids in porous media: Dover, New York.

Bedford, A., Costley, R. D., & Stern, M. (1984). On the drag and virtual mass coefficients in Biot's equations. *Journal of the Acoustical Society of America, 76*, 1804–1809.

Biot, M. A. (1956a). Theory of propagation of elastic waves in a fluid-saturated porous solid. I. Low-frequency range. *Journal of the Acoustical Society of America, 28*, 168–178.

Biot, M. A. (1956b). Theory of propagation of elastic waves in a fluid-saturated porous solid. II. Higher-frequency range. *Journal of the Acoustical Society of America, 28*, 179–191.

Biot, M. A. (1962a). Generalized theory of acoustic propagation in porous dissipative media. *Journal of the Acoustical Society of America, 34*, 1254–1264.

Biot, M. A. (1962b). Mechanics of deformation and acoustic propagation in porous media. *Journal of Applied Physics, 33*, 1482–1498.

Biot, M. A., & Willis, D. G. (1957). The elastic coefficients of the theory of consolidation. *Journal of Applied Mechanics, 24*, 594–601.

Brown, R. J. S. (1980). Connection between formation factor for electrical resistivity and fluid-solid coupling factor in Biot's equations for acoustic waves in fluid-filled porous media. *Geophysics, 45*, 1269–1275.

Clennell, M. B. (1997). Tortuosity: a guide through the maze. In *Developments in petrophysics, Geological Society Special Publication 122*, M. A. Lovell & P. K. Harvey (Eds.): London, 299–344.

Geertsma, J. (1961). Velocity-log interpretation: the effect of rock bulk compressibility. *Society of Petroleum Engineers Journal*, December, 235–246.

Goldberg, I., & Gurevich, B. (1998). A semi-empirical velocity-porosity-clay model for petrophysical interpretation of P- and S-velocities. *Geophysical Prospecting, 46*, 271–285.

Gurevich, B., Kelder, O., & Smeulders, D. M. J. (1999). Validation of the slow compressional wave in porous media: comparison of experiments and numerical simulations. *Transport in Porous Media, 36*, 149–160.

Hovem, J. M., & Ingram, G. D. (1979). Viscous attenuation of sound in saturated sand. *Journal of the Acoustical Society of America, 66*, 1807–1812.

Johnson, D. L. (1980). Equivalence between fourth sound in liquid He II at low temperatures and the Biot slow wave in consolidated porous media. *Applied Physics Letters, 37*, 1065–1067.

Johnson, D. L., Hemmick, D. L., & Kojima, H. (1994a). Probing porous media with first and second sound. I. Dynamic permeability. *Journal of Applied Physics, 76*, 104–114.

Johnson, D. L., Koplik, J., & Dashen, R. (1987). Theory of dynamic permeability and tortuosity in fluid-saturated porous media. *Journal of Fluid Mechanics, 176*, 379–402.

Johnson, D. L., Plona, T. J., & Kojima, H. (1994b). Probing porous media with first and second sound. II. Acoustic properties of water-saturated porous media. *Journal of Applied Physics, 76*, 115–125.

Johnson, D. L., Plona, T. J., Scala, C., Pasierb, F., & Kojima, H. (1982). Tortuosity and acoustic slow waves. *Physical Review Letters, 49*, 1840–1844.

Krief, M., Garat, J., Stellingwerff, J., & Ventre, J. (1990). A petrophysical interpretation using the velocities of P and S waves (full waveform sonic). *The Log Analyst, 31*, 355–369.

Landau, L. D., & Lifshitz, E. M. (1959). Fluid mechanics: Pergamon Press.

Mavko, G., Mukerji, T., & Dvorkin, J. (2009). The rock physics handbook (2nd ed.). New York: Cambridge University Press.

Molotkov, L. A. (2002). On the coefficients of pore tortuosity in the effective Biot model. *Journal of Mathematical Sciences, 108*, 752–757.

Stoll, R. D. (1974). Acoustic waves in saturated sediments. In *Physics of sound in marine sediments*, L. Hampton (Ed.). New York: Plenum Press, 19–39.

Stoll, R. D. (1977). Acoustic waves in ocean sediments. *Geophysics, 42*, 715–725.

Zhou, M.-Y., & Sheng, P. (1989). First-principles calculations of dynamic permeability in porous media. *Physical Review B, 39*, 12027–12039.

Zwikker, C., & Kosten, C. W. (1949). Sound absorbing materials. New York: Elsevier.

(Received September 3, 2015, revised June 7, 2016, accepted July 5, 2016, Published online July 23, 2016)